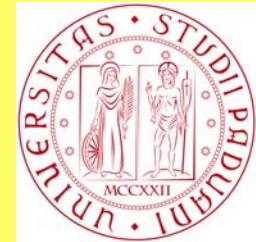


The nature of gas and stars in the circumnuclear regions of AGN: a chemical approach.

Piero Rafanelli

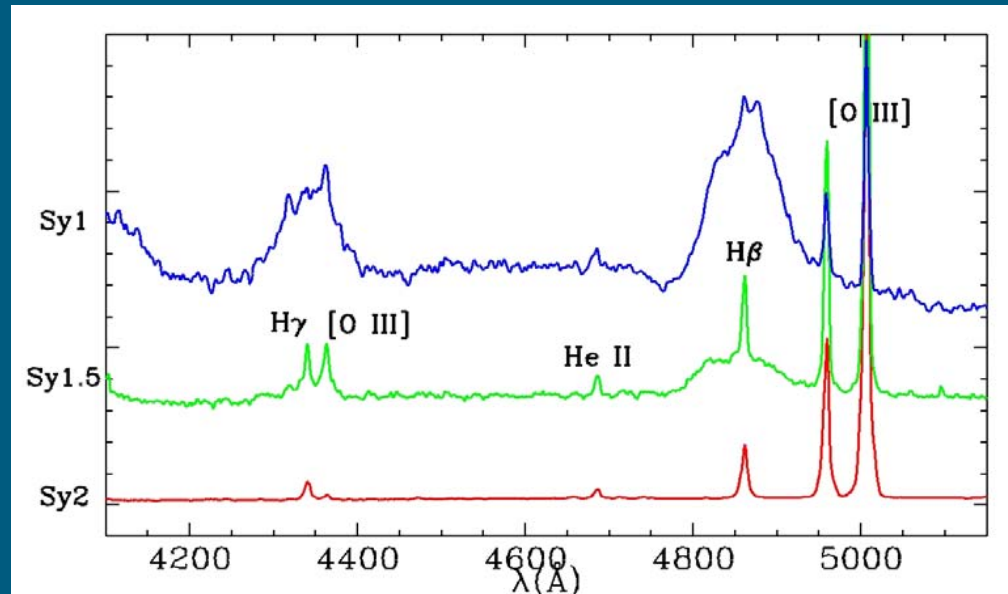
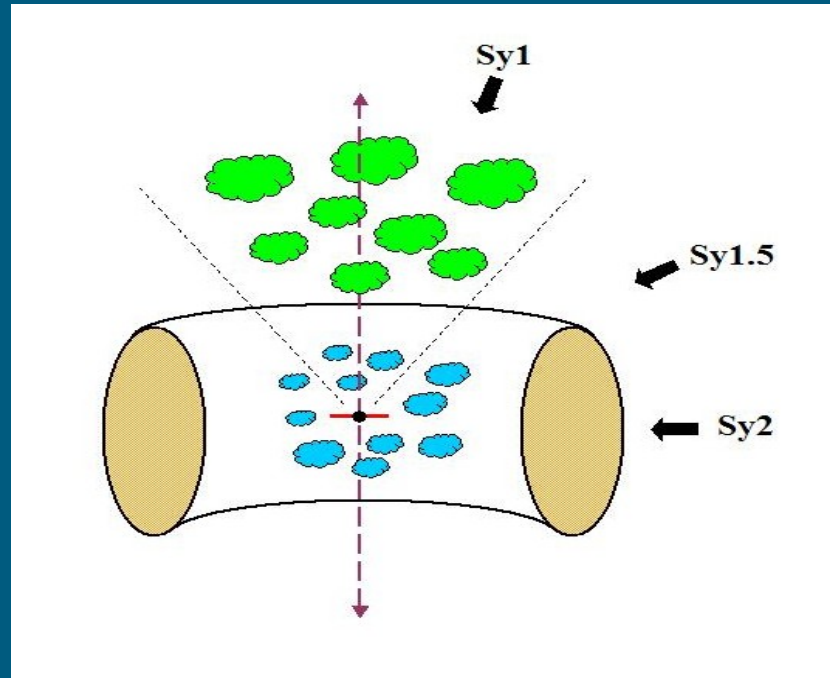
Department of Astronomy
University of Padova



L. Vaona
R. D'Abrusco
S. Cirio
V. Cracco

- Aim of this communication is to present the first results of a work-in-progress regarding the chemical properties (abundance of elements) of gas and stars in the circumnuclear regions of AGN.
- It has been often suggested that nuclear and circumnuclear **Star Formation activity** and **Seyfert activity** can be connected in an **evolutive sequence and/or coexist**, like verified in many objects.
- In order to verify the reliability of this idea based essentially on detailed observations of **single objects**, we have recently analyzed the circumnuclear stellar continua of large samples of S2, SFG and NG for finding whether the stellar populations therein show signatures which can support this scenario. The results of such investigation have clearly demonstrated the **presence in S2 of an excess of A stars** compared to NG, which witnesses a history of **past recent star formation**.
- A further step in this investigation, aimed to strengthen these results, has been to address our attention to
 1. the **chemical composition of circumnuclear gas**, namely the **humus** where the stars are located in S2 and SFG;
 2. the **metal abundances and ages of stars** in the circumnuclear region of S2, SFG and NG

Unified Model



Selection of the emission line galaxies

A sample of 119226 emission line galaxies has been extracted from SDSS–DR7 spectroscopic survey (fiber size 3 arcsec) imposing to their spectra to match the following conditions:

- 1) Presence of the emission lines:
[OIII] λ 5007,
[OII] $\lambda\lambda$ 3728-3729 ,
[OI] λ 6300.
- 2) S/N > 3 of the [OI] λ 6300 line.

Different families of emission line galaxies have been selected using:

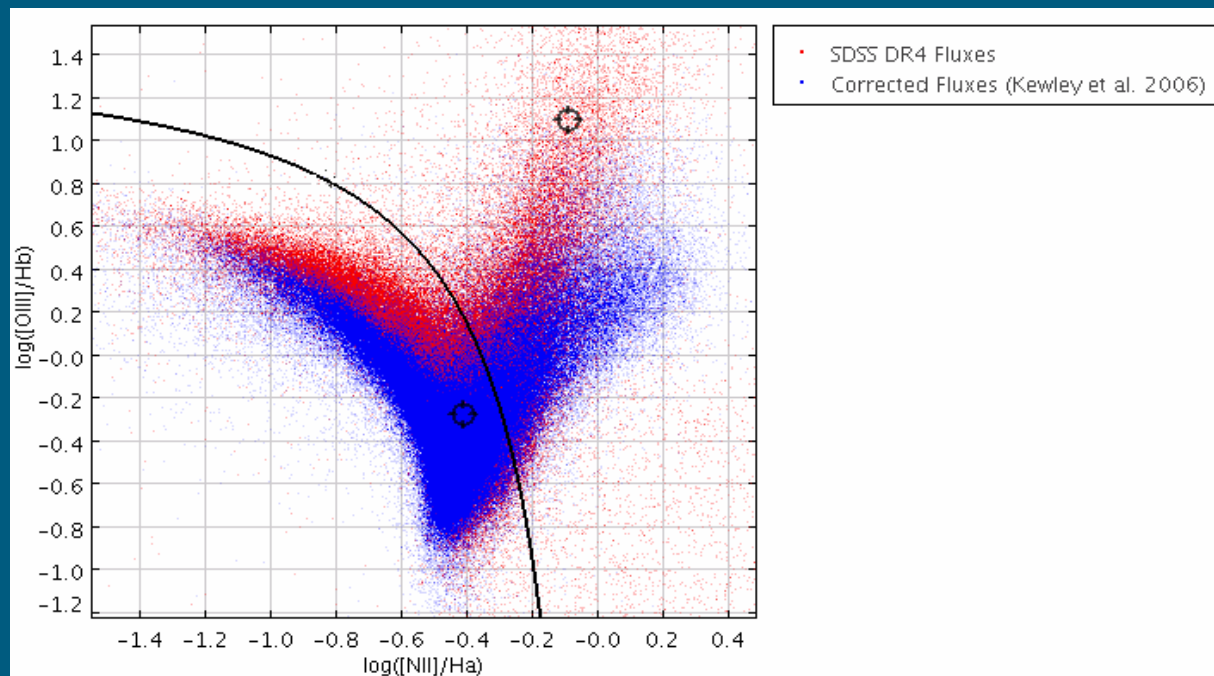
- the classical Veilleux, Osterbrock (VO) diagnostic diagrams.

In the VO diagrams we have used the parametrization of the borderlines between AGNs and star-forming galaxies (SFs) introduced by Kewley et al., 2006.

Effects of the subtraction of the galactic component

The diagnostic line ratios, like $[\text{NII}]6548\text{-}83/\text{H}\alpha$ - $[\text{OIII}]5007/\text{H}\beta$ etc., have been derived measuring the intensity of the emission lines after subtraction of the stellar component from the spectra of the selected galaxies. This procedure allows to avoid the influence of the underlying absorption component in the determination of the intensity of the recombination lines. The effects of such subtraction are shown in the following figure, obtained analyzing the data published by Kewley et al. (2006).

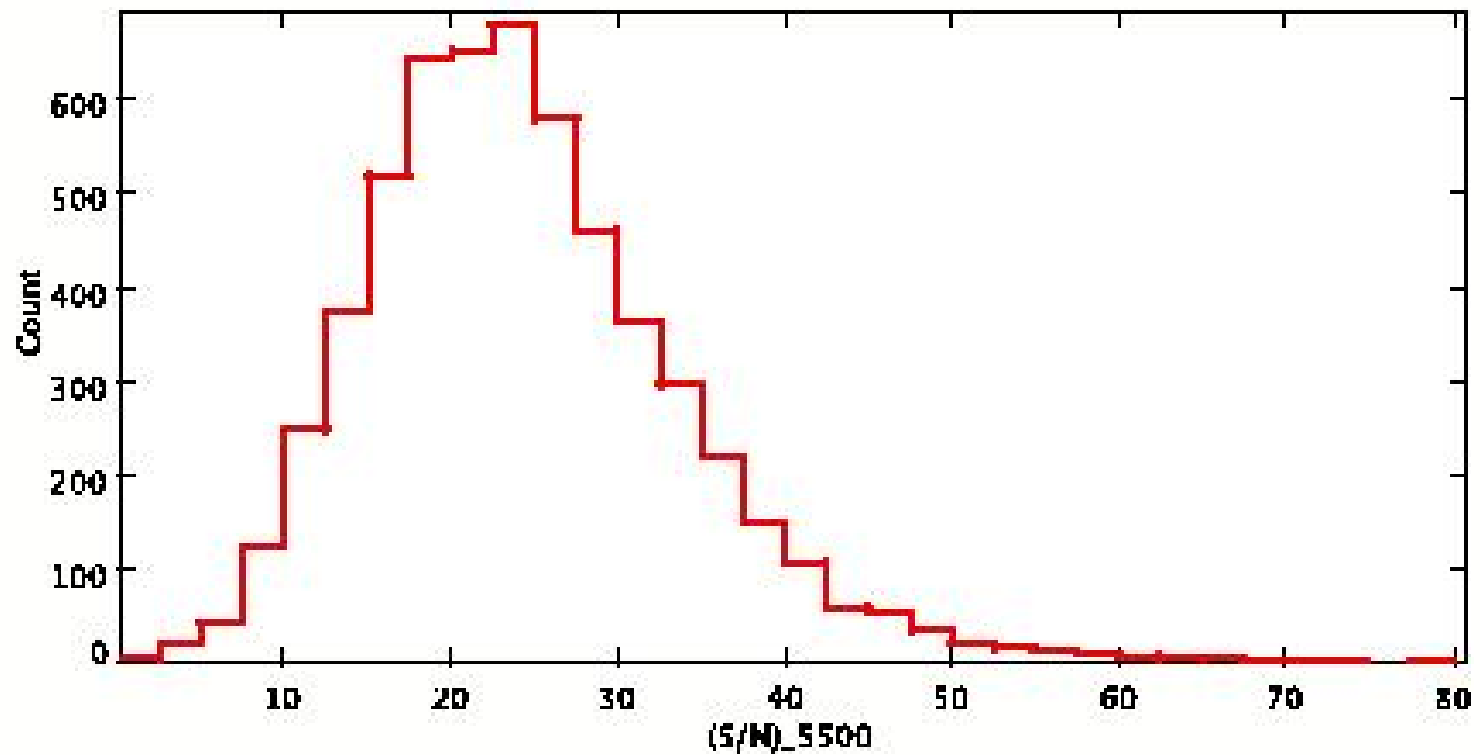
As an example, it is shown that the point representing the line ratios of an object moves from top to bottom and from right to left after subtraction of the galactic stellar component.



SEYFERT-2 and Star-forming galaxies

- In the range $0.04 < z < 0.1$ (2.4-4.8 kpc within 3 arcsec aperture) we find **3064 AGNs** and **44606 SFG** (in the range $0.04 < z < 0.08$).
- The AGN have been corrected for the underlying continuum using STARLIGHT (Cid Fernandes et al 2005) and we have measured the fluxes of all lines with $S/N > 5$
- With multiple Gaussian fits we have isolated the sources having only narrow line profiles and classified as S2 in the VO diagnostic diagrams. We obtained in this way our final sample of **2153 S2** galaxies

Distribution of the S/N ratio of the continua of S2 galaxies at $\lambda = 5500 \text{ \AA}$.

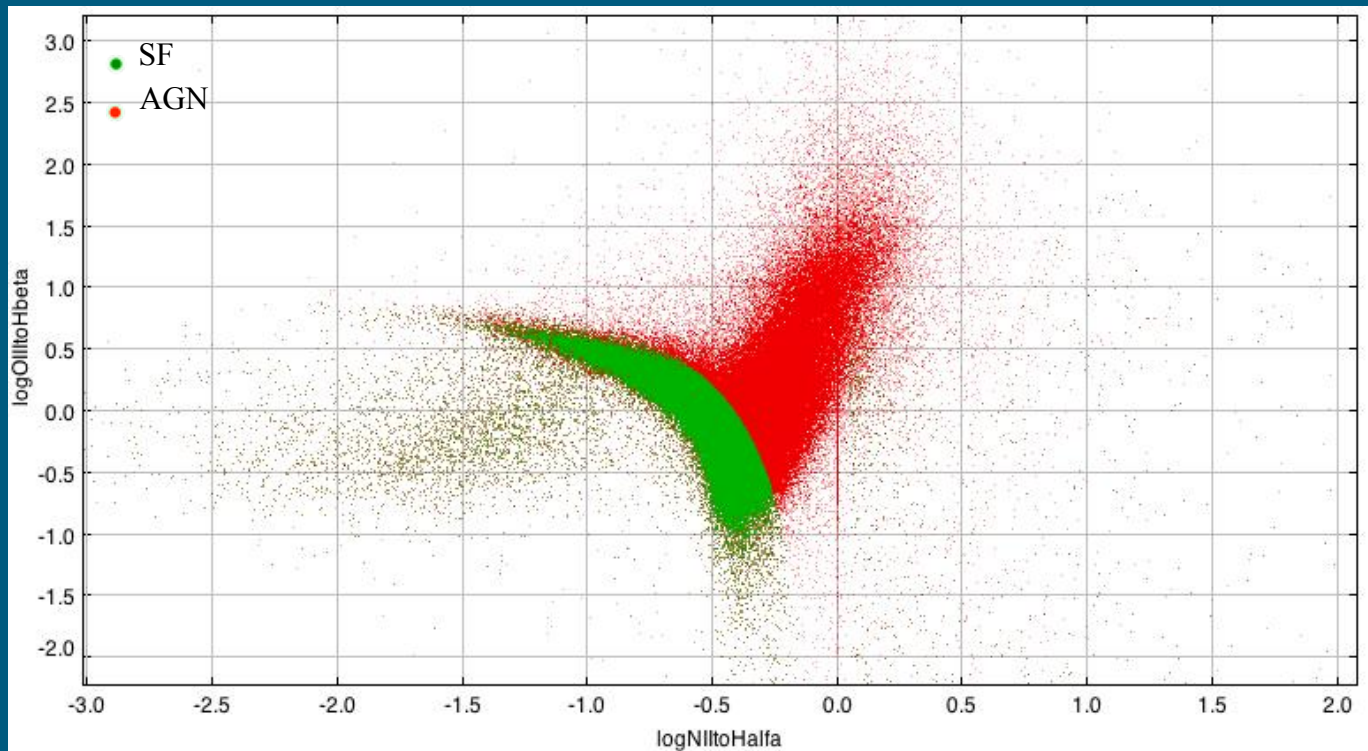


1302 SFG galaxies ($S/N > 10$ on the continuum at $\lambda = 5500 \text{ \AA}$) have been selected from the previous sample using the VO diagrams and imposing the following conditions:

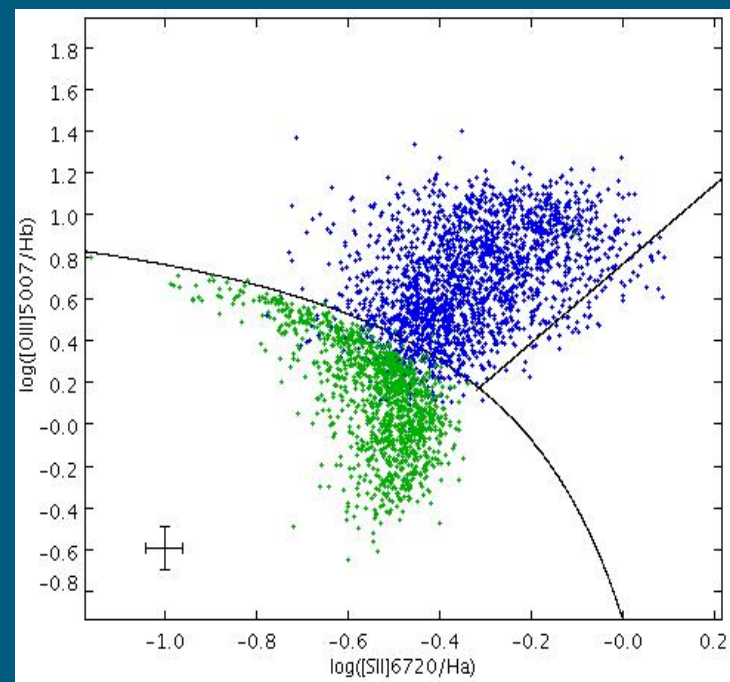
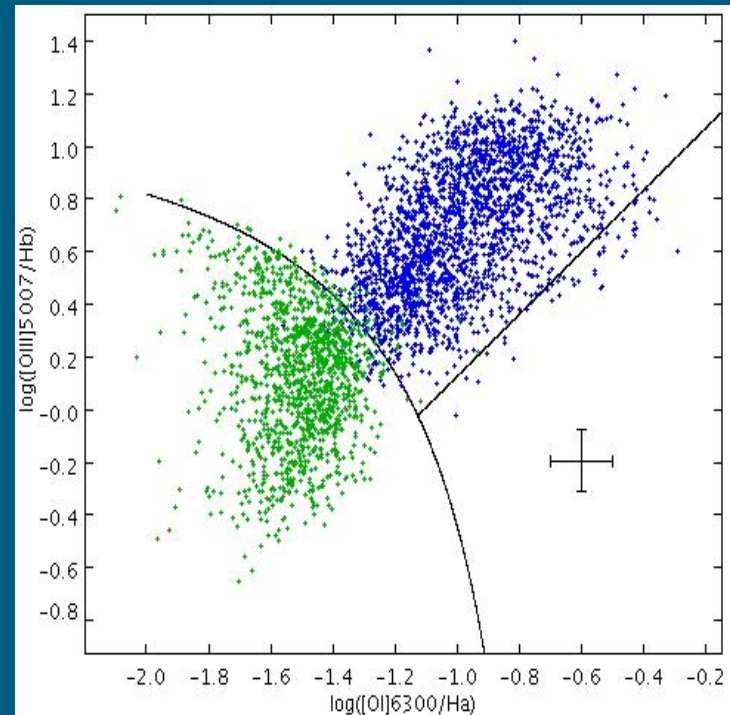
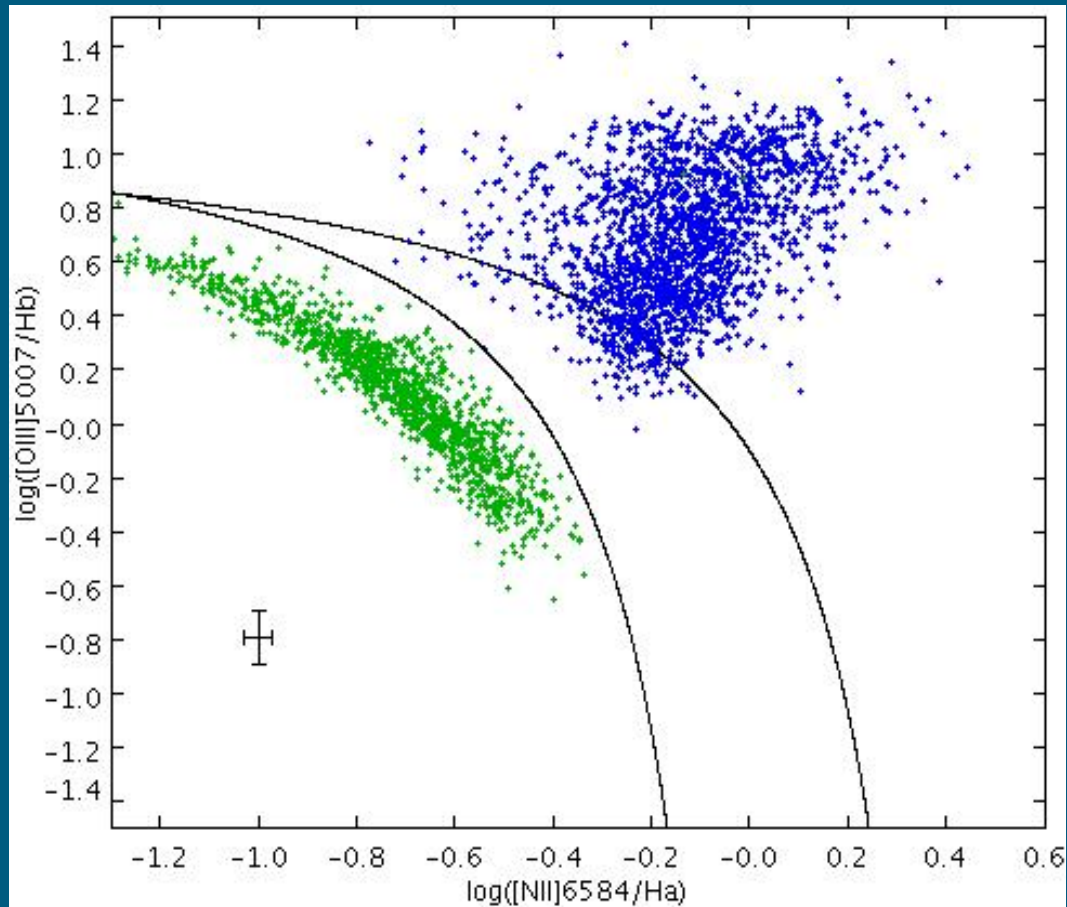
$$\log([\text{OIII}]/\text{H}\beta) < 0.61/[\log([\text{NII}]/\text{H}\alpha)] + 1.3$$

$$\log([\text{OIII}]/\text{H}\beta) < 0.72/[\log([\text{SII}]/\text{H}\alpha)] + 1.3$$

$$\log([\text{OIII}]/\text{H}\beta) < 0.73/[\log([\text{OI}]/\text{H}\alpha)] + 1.33$$

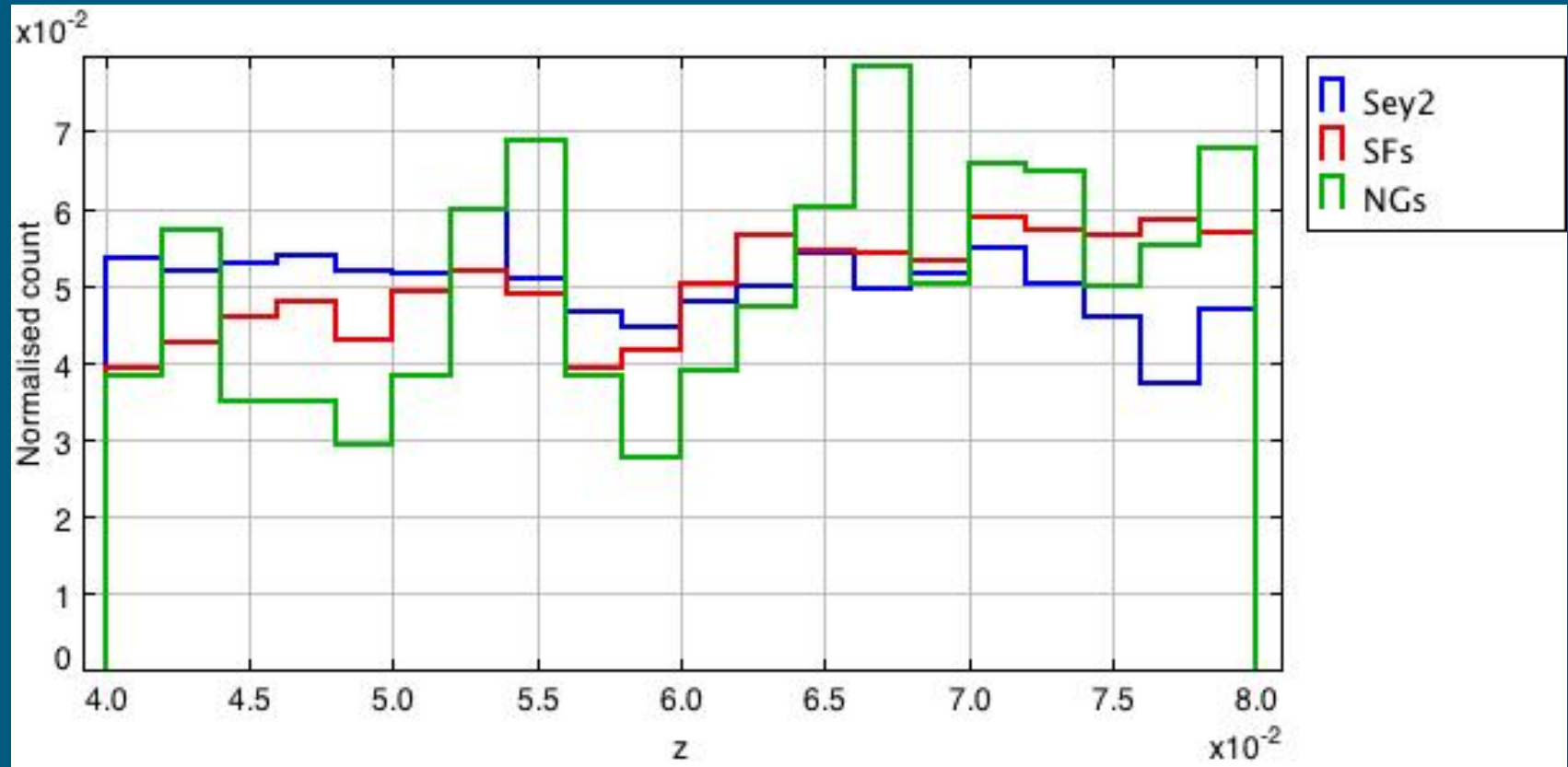


Final samples



Normal galaxies

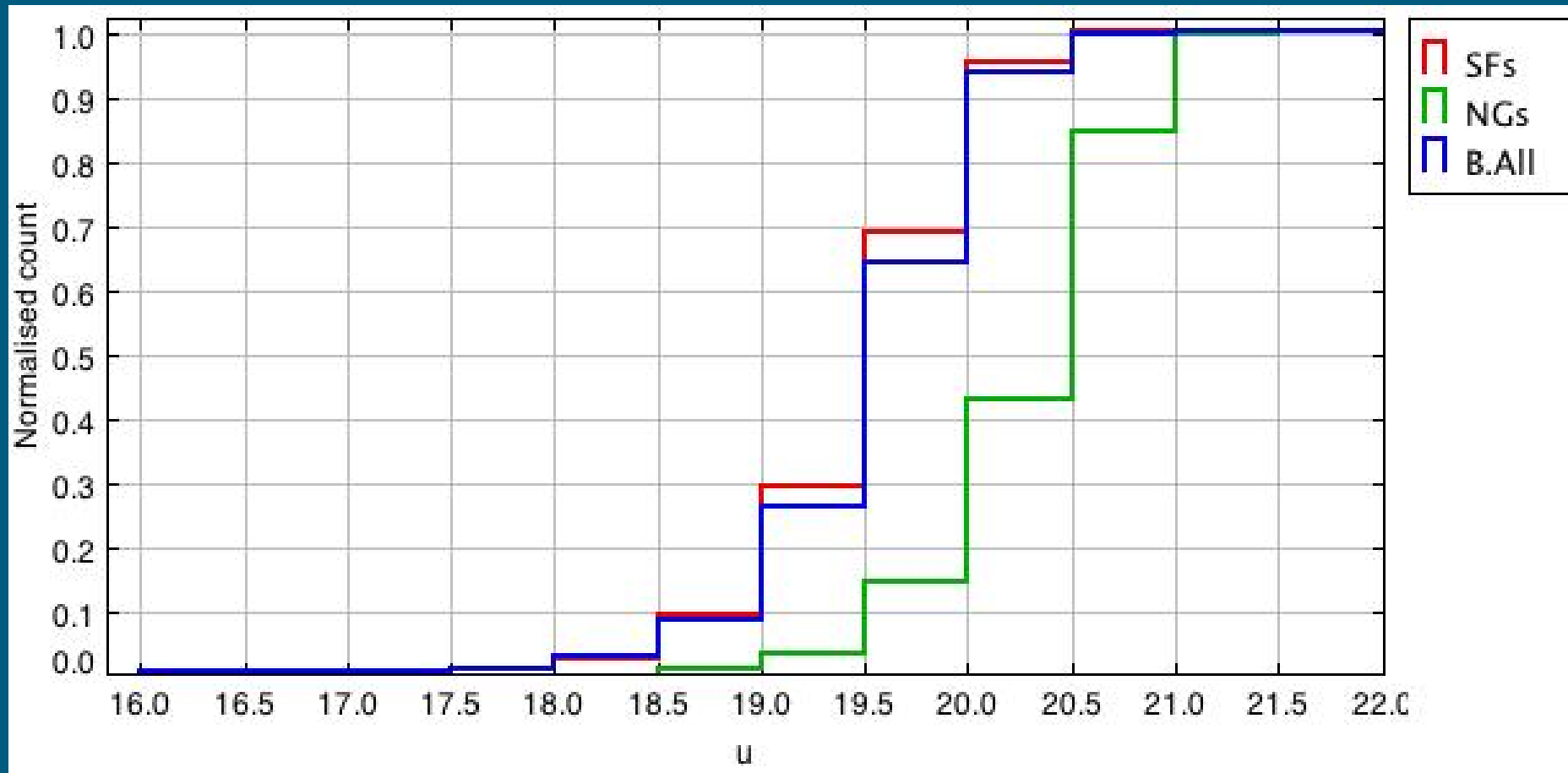
2000 normal galaxies (NG) with $0.04 < z < 0.08$ and $S/N > 10$ on the continua at $\lambda = 5500 \text{ \AA}$ have been extracted from the SDSS catalogue



Redshift distribution in the $[0.04, 0.08]$ interval for the three samples.

Cumulative magnitude distribution

Cumulative u magnitude (magnitude within $1 R_p$) distribution for the three samples.



SDSS morphology

SDSS galaxies photometric profiles are fitted with three different models: De Vaucouleurs' law, Exponential Profile, PSF.

For each of these models, a likelihood is calculated, so that a **rough morphological** classification can be obtained by evaluating the **fractional likelihoods** for each photometric model:

$$\text{fracLik_DeV} = \log\text{Lik_DeV} / (\log\text{Lik_DeV} + \log\text{Lik_Exp} + \log\text{Lik_PSF})$$

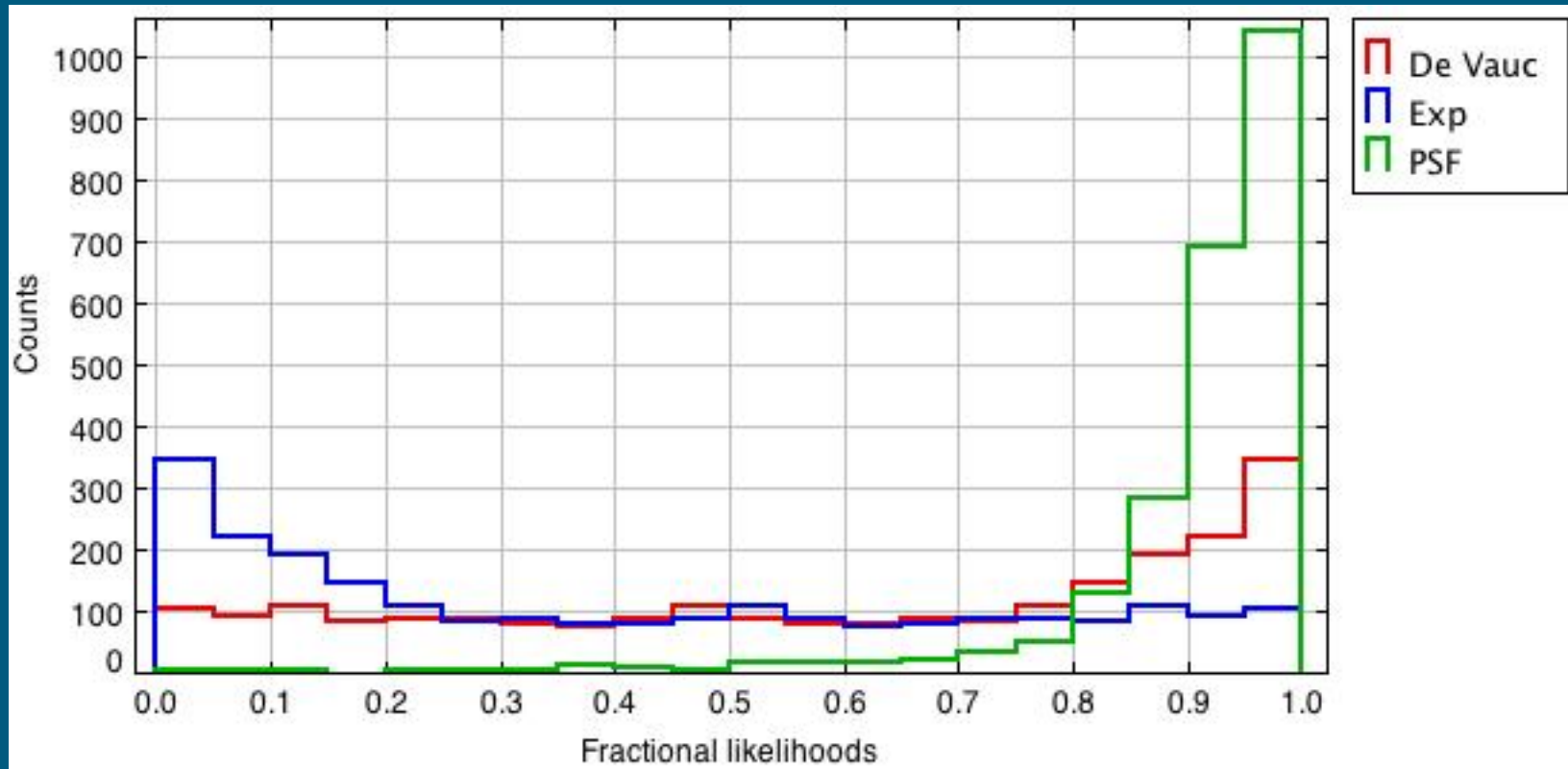
$$\text{fracLik_Exp} = \log\text{Lik_Exp} / (\log\text{Lik_DeV} + \log\text{Lik_Exp} + \log\text{Lik_PSF})$$

$$\text{fracLik_PSF} = \log\text{Lik_PSF} / (\log\text{Lik_DeV} + \log\text{Lik_Exp} + \log\text{Lik_PSF})$$

fracLik = fractional **Likelihood**

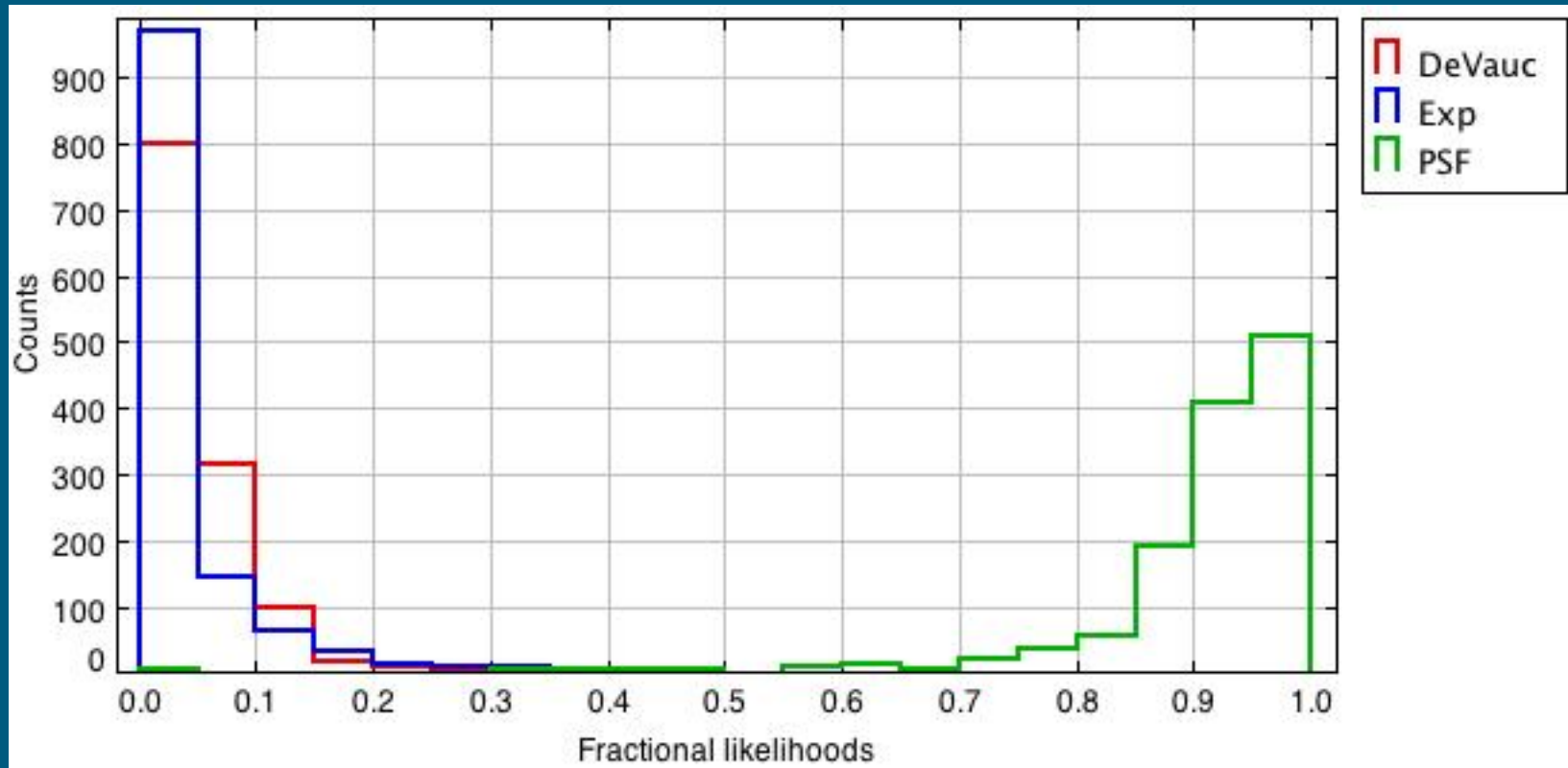
Seyfert 2 morphology

Morphology of Sey2 galaxies according to the SDSS photometric fractional likelihoods of DeV, Exp and PSF models (u band):

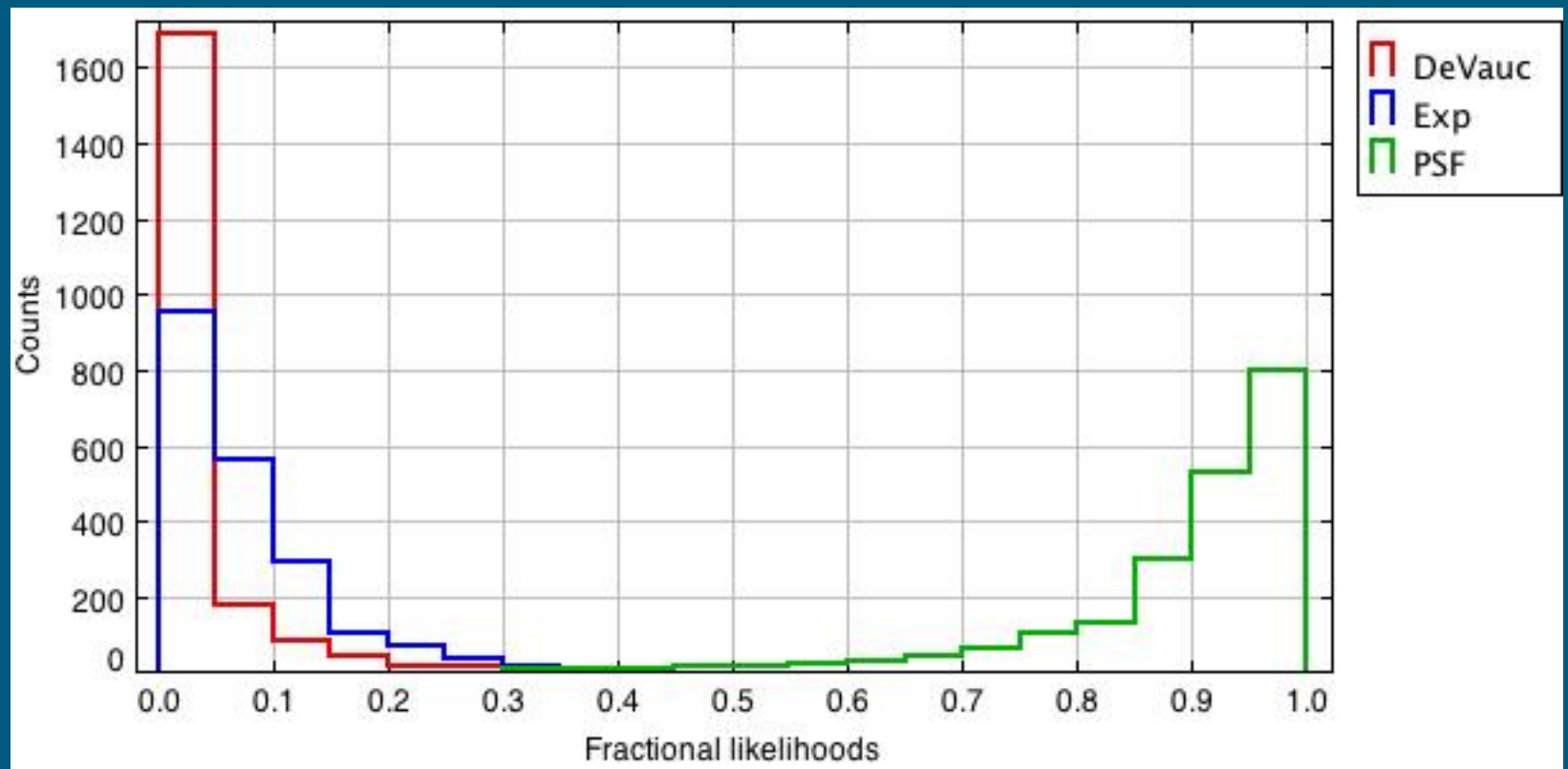


SFG galaxies vs SDSS morphology

Morphology of SFs galaxies according to the SDSS photometric fractional likelihoods of DeV, Exp and PSF models (u band):



NGs SDSS morphology

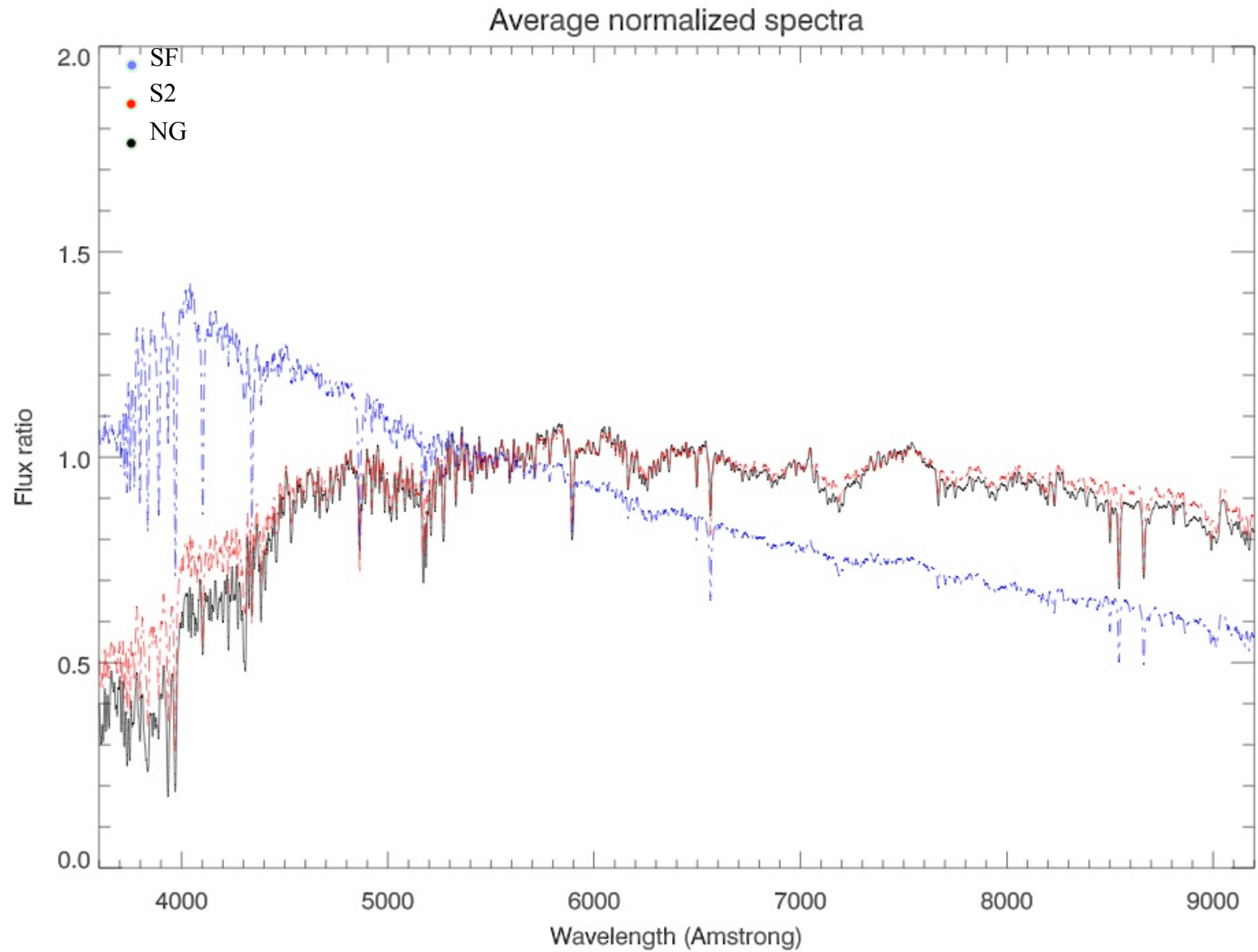


STELLAR CONTINUUM

The observed spectra of all galaxies have been analyzed using the code STARLIGHT (Cid Fernandes et al. 2005) which fits the observed spectrum using a linear combination of simple theoretical stellar populations (coeval and chemically homogeneous) computed with evolutionary synthesis models at the same spectral resolution as that of the SDSS.

In this way we have reproduced the stellar spectrum of all our galaxies: S2, SFG, NG.

Average spectra



S2 / NG ratio (average of all galaxies)

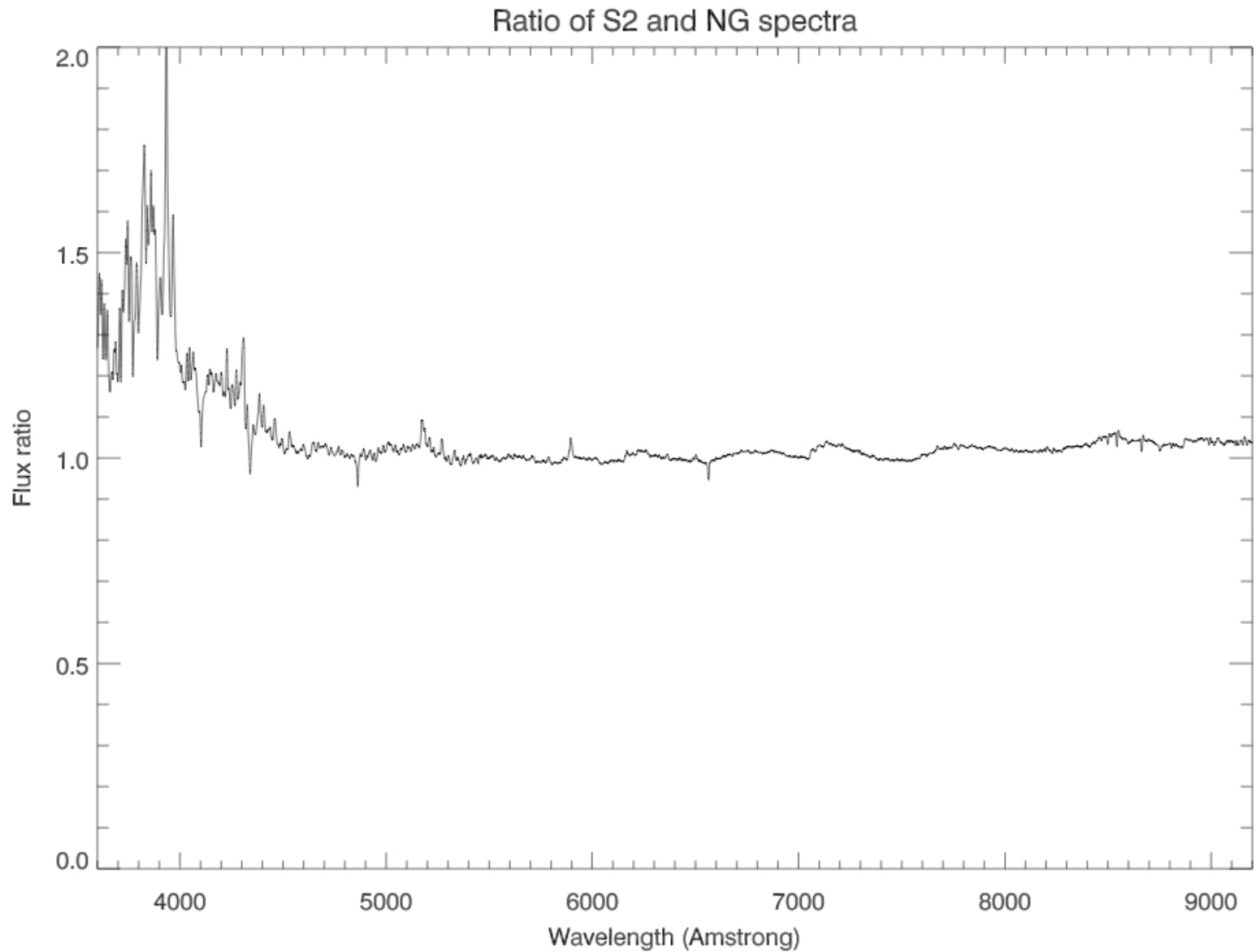


Photo-ionization models of the NLR of S2

Input Parameters

Single cloud



Two clouds

Metallicity Z in solar unit
photoionization power-law index α
ionization parameter U
density n_e [cm^{-3}]
column density $n_c(\text{H}^+)$ [cm^{-2}]
Dust/Gas properties in Galactic units

Lines to reproduce

<u>Ion</u>	<u>λ (Å)</u>	
[O II]	3727	doublet
[Ne III]	3869	
[NeIII]	3968	
[S II]	4070	doublet
H δ	4102	
H γ	4340	
[O III]	4363	
He II	4686	
[Ar IV]	4711	
[Ar IV]	4740	
H β	4861	
[O III]	4959	
[O III]	5007	
[N I]	5199	
[Fe VII]	5720	
He I	5876	
[Fe VII]	6087	
[O I]	6300	
[N II]	6548	
H α	6563	
[N II]	6583	
[S II]	6716	
[S II]	6731	
[Ar III]	7136	
[O II]	7325	doublet

Single cloud models

In order to define a grid of models, we have combined the following set of values of the input parameters of the photoionization code CLOUDY, which should reproduce the observed line fluxes of the emission lines listed in the table here on the left side

$Z = 0.5 \rightarrow 3.5$ step 0.5

$\alpha = -1.0, -1.3, -1.6, -1.9, -2.2$

$\log(U) = -1.6, -2.0, -2.4, -2.8, -3.2, -3.6$

$\log(n_e [\text{cm}^{-3}]) = 1.0, 1.5, 2.0, 2.5, 3.0, 3.5, 4.0$

$\log n_c (\text{H}^+) [\text{cm}^{-2}] = 19.0 \rightarrow 22.2$ step 0.4

Dust/Gas = 0.25, 0.50, 0.75, 1.00 ISM

total number of single cloud models 37401

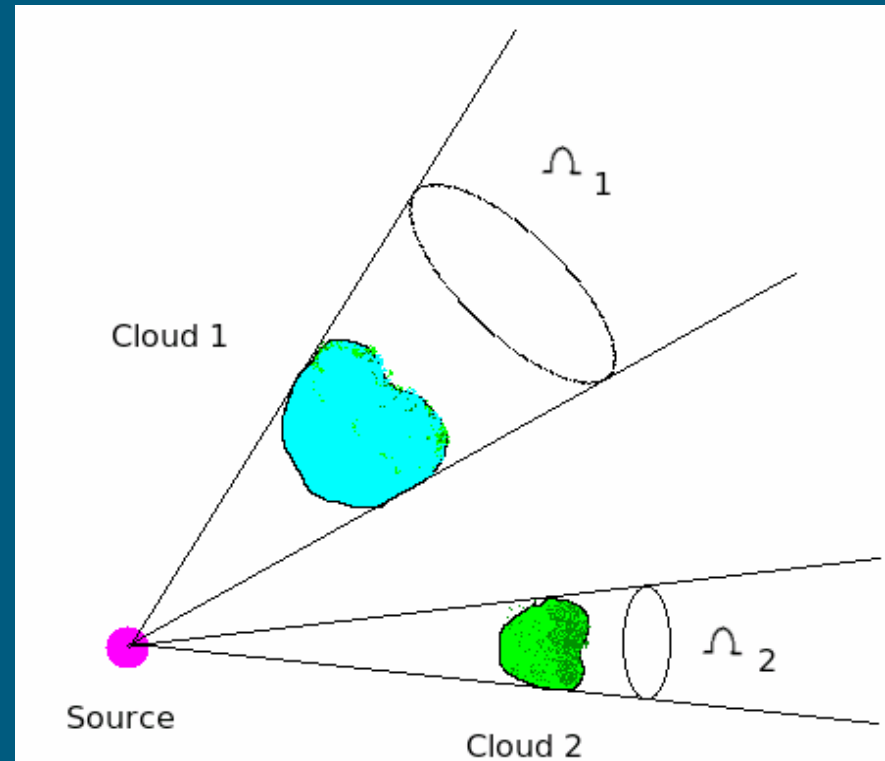
Two clouds models

Assuming the presence of two clouds, all the possible combinations between two single models with fixed photoionization index (α), Dust/Gas and metallicity were considered.

A further parameter is the geometrical factor, the ratio of the solid angle subtended from each cloud respect to the source. Five different values were adopted for this parameter, $\Omega_1/\Omega_2=0.25, 0.5, 1, 2, 4$

Only the models which satisfy the Veilleux and Osterbrock diagrams, following the Kewley conditions, are accepted.

The total number of accepted models is **9361629**



The comparison

In order to compare the observed spectra with the models the χ^2 test was performed. The degrees of freedom, necessary in order to define the significance level of acceptability, is given by the difference between the number of measured lines and the number of parameters employed in the models.

Single models 8 parameters

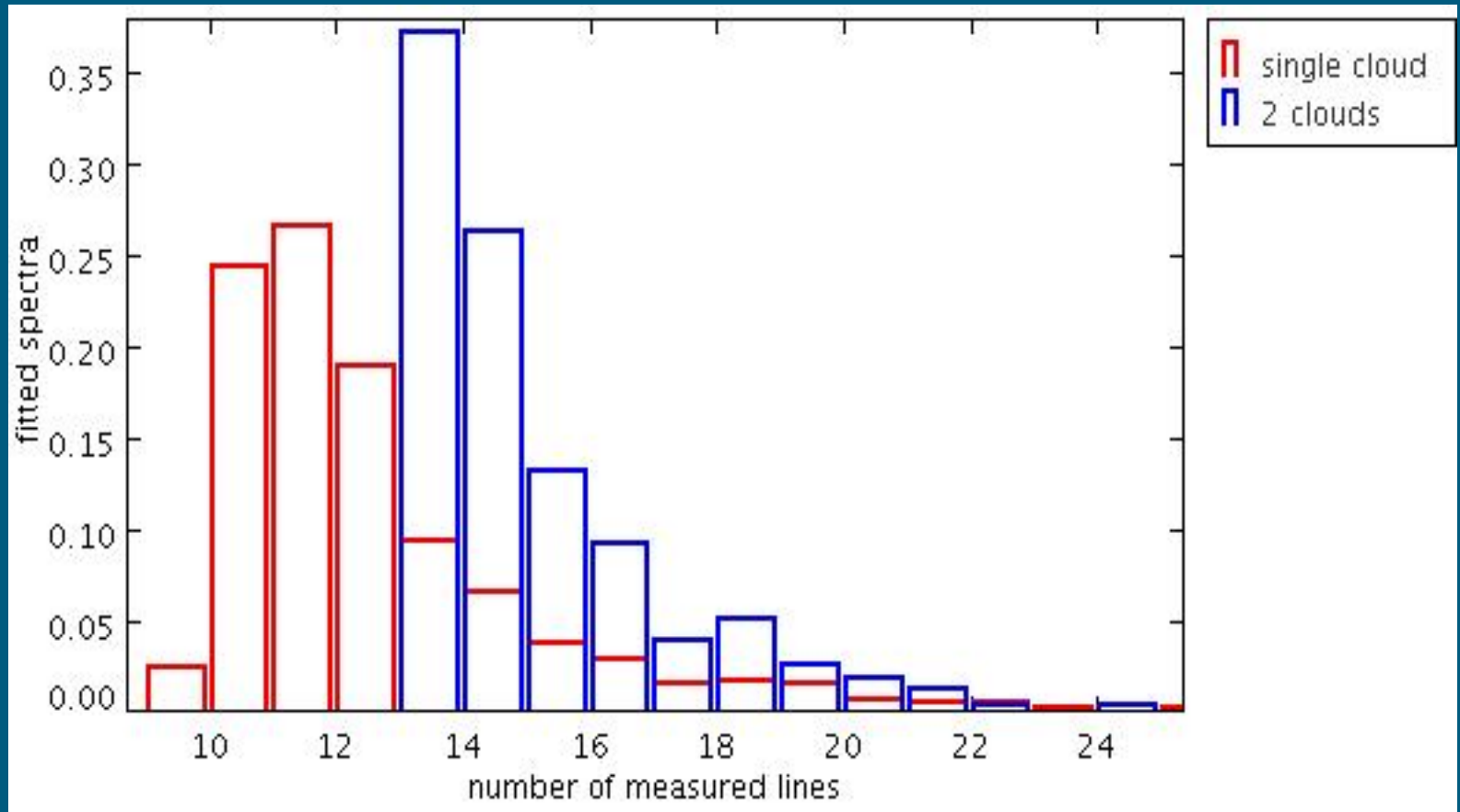
Two clouds models 12 parameters.

It means that the minimum number of measured lines must be at least 9 for the single cloud and 13 for two clouds models.

It means that all the sample is comparable with the single models but only 607 spectra of the whole sample can be taken into account for the comparison with 2 clouds models.

Fitted spectra:

Two-clouds models need many measured lines but are able to fit these spectra!



The χ^2 test was performed comparing the measured fluxes with those obtained by CLOUDY, after having applied a galactic extinction in order to match the observed H α /H β ratio .

This choice permits to compare directly the fluxes without assuming a theoretical H α /H β ratio.

About 9 different values of A_V for each spectrum were calculated comparing the H α /H β observed ratio (keeping into account the errors) with the H α /H β calculated ratio. Then the χ^2 was calculated as

$$\chi_{\lambda}^2 = \frac{(F(\lambda)_{OBS} - F(\lambda)_{CLOUDY})^2}{(2 \cdot \sigma_{\lambda})^2}$$

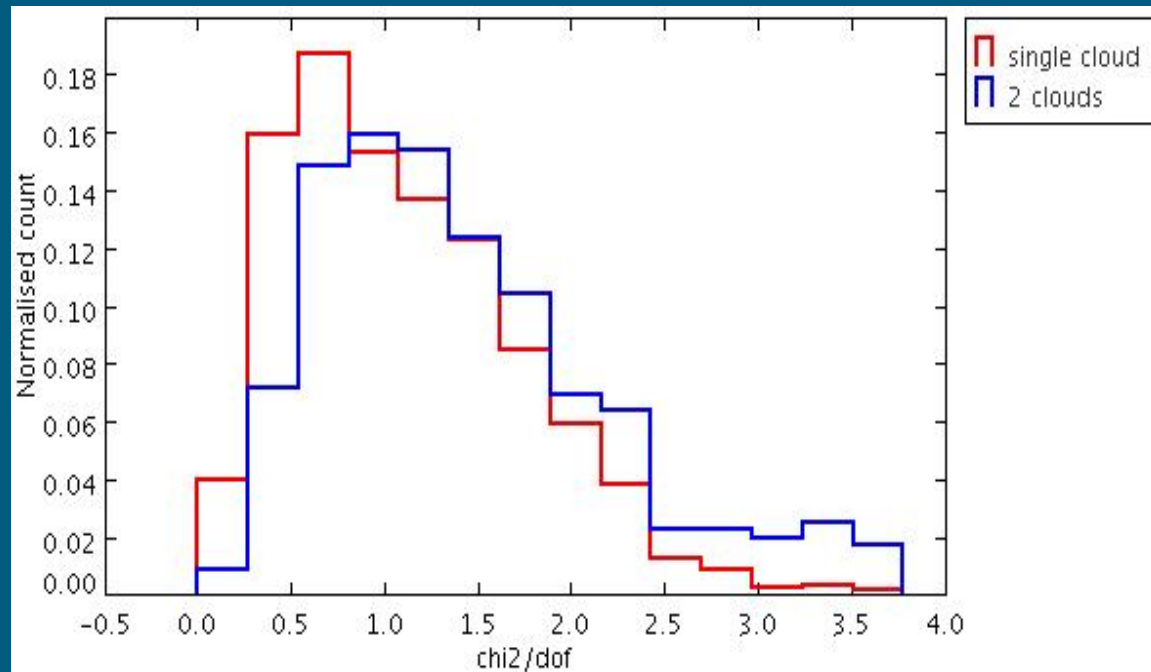
The choice of 2σ is suggested by the χ^2 distribution analysis, while 1σ is a slight underestimate of the fitting whereas 3σ is an absolute overestimate.

Goodness of the fit

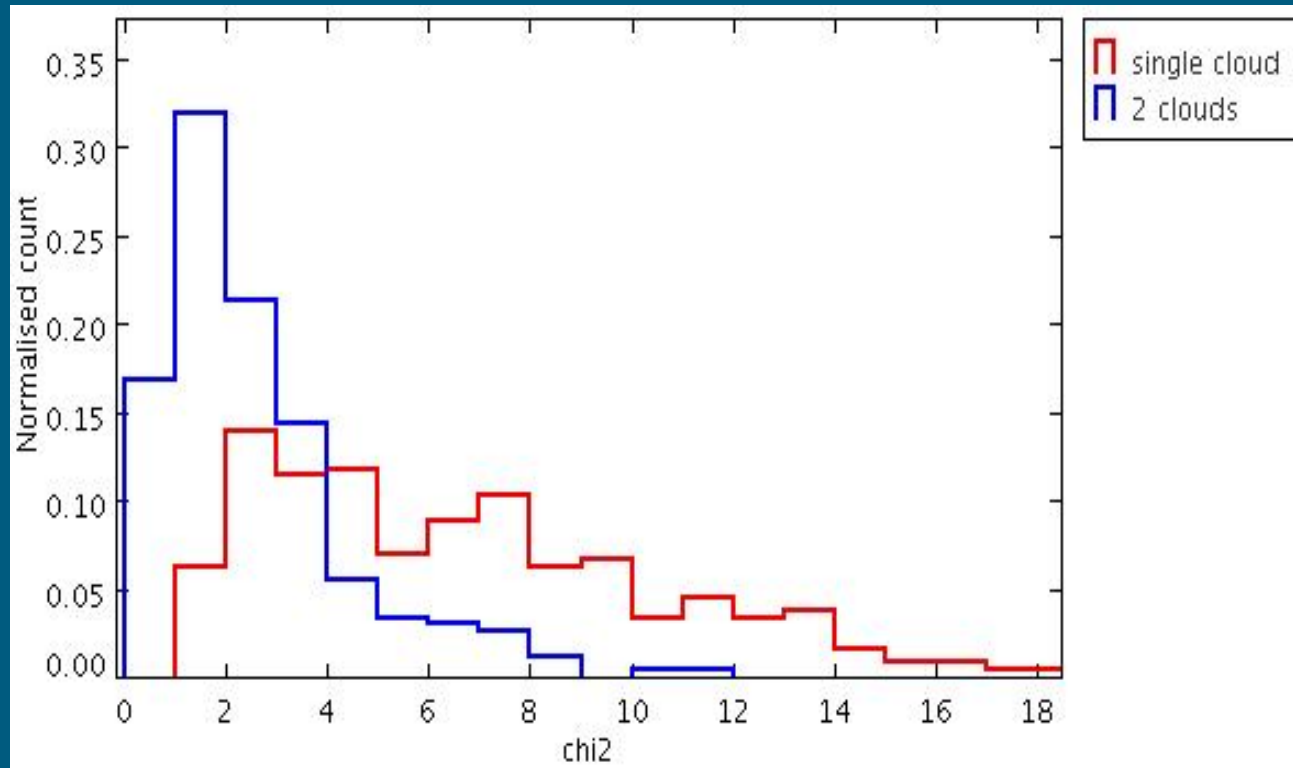
5% of significance:

single models 76% → no good χ^2/dof distribution,
well fitted spectra with a low number
of reliably measured lines

2 clouds models 60% → good χ^2/dof distribution



χ^2 absolute distribution of the same fitted objects
(60% of the 607 S2 = 366) :
the match between single and 2 clouds models



Chemical abundance

method

Star-forming galaxies

empirical calibration: P method

(Pilyugin & Thuan, 2005)

Seyfert 2 galaxies

photo-ionization models

(Vaona PhD thesis, 2009)

Normal galaxies

Mg_2 index

(Bender et al., 1993)

Star-forming galaxies

Since 1979 (Pagel et al 1979) it was found that the ratio

$$R_{23} = \frac{([OII] \lambda 3727 + [OIII] \lambda 4959,5007)}{(H\beta)}$$

depends on the Oxygen abundance.

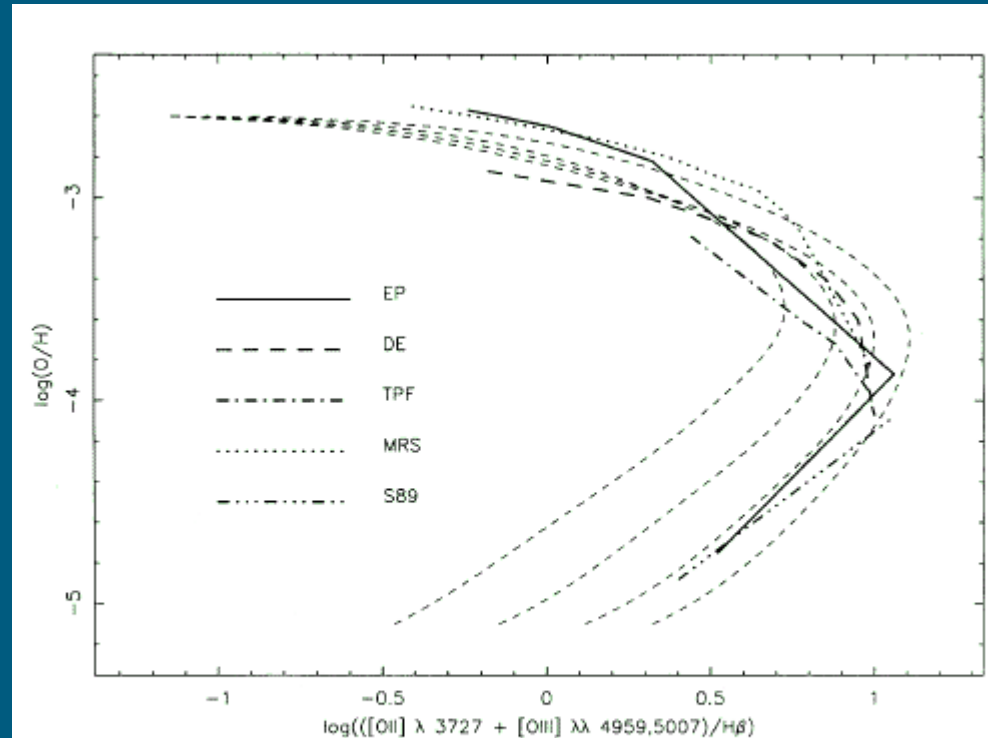


FIG. 11.—Comparison of previous calibrations of R_{23} to that presented here. For clarity, only models with $M_u = 60 M_\odot$ are plotted here. Other lines are as per Fig. 1.

Pilyugin (2000, 2001) introduced the excitation parameter P defined as

$$P = \frac{([OIII]4959,5007)}{([OII]3727 + [OIII]4959,5007)}$$

then a more general two-dimensional parametric calibration of the functional form $O/H = f(P, R_{23})$ was obtained.

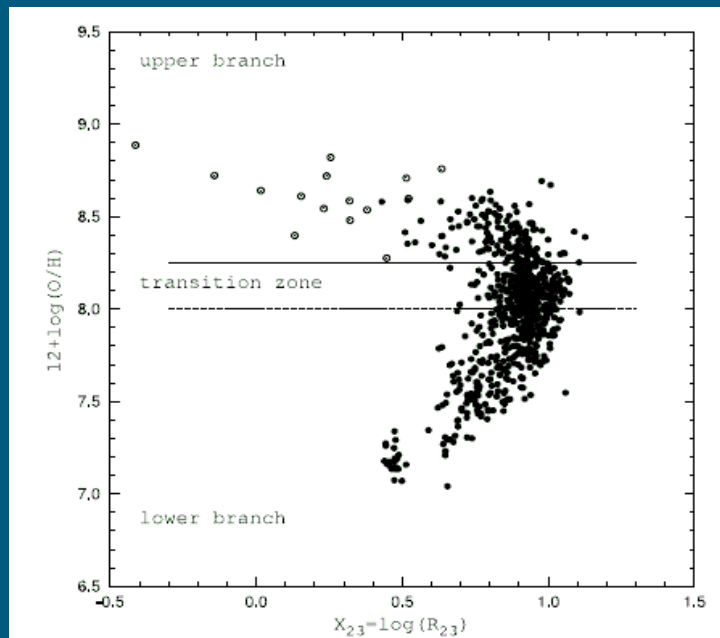


FIG. 2.— R_{23} -O/H diagram. Filled circles are H II regions from our total sample listed in Table 1, and open circles are low-excitation H II regions from Bresolin et al. (2004); Kennicutt et al. (2003); Castellanos et al. (2002). Horizontal lines show the adopted boundaries between the lower branch and the transition zone (dashed line) and between the upper branch and the transition zone (solid line).

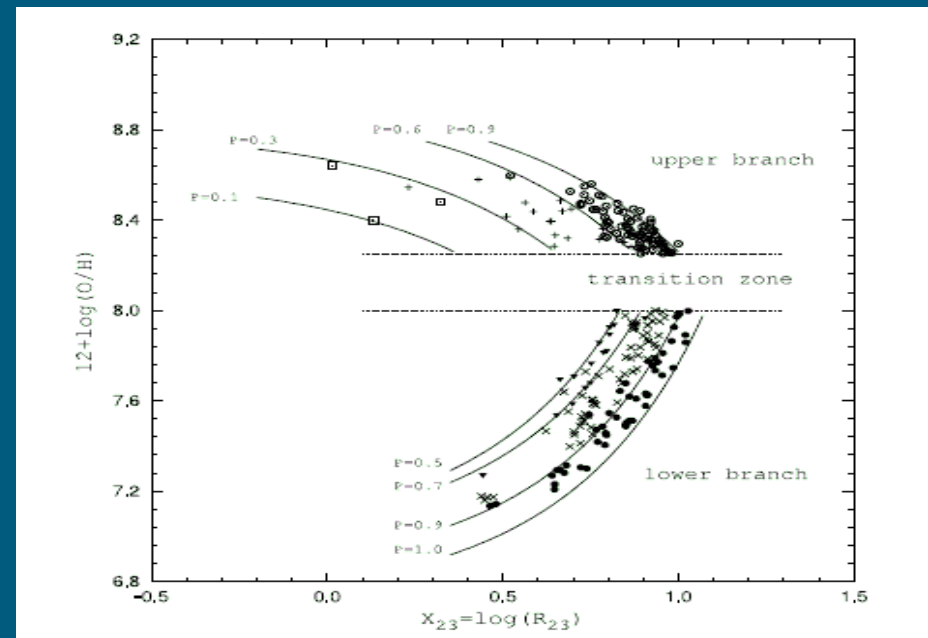


FIG. 12.—Family of $O/H = f(R_{23}, P)$ curves labeled by different values of the excitation parameter P , superimposed on the observational data. The high-metallicity H II regions with $0.0 < P < 0.3$ are shown by open squares, those with $0.3 < P < 0.6$ by plus signs, and those with $0.6 < P < 0.9$ by open circles. The low-metallicity H II regions with $0.5 < P < 0.7$ are shown by filled triangles, those with $0.7 < P < 0.9$ by crosses, and those with $0.9 < P < 1.0$ by filled circles.

Our sample is placed in the upper branch.

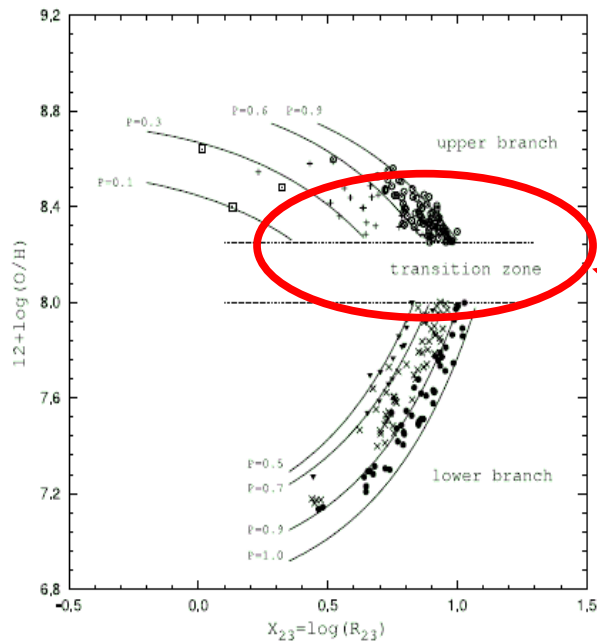
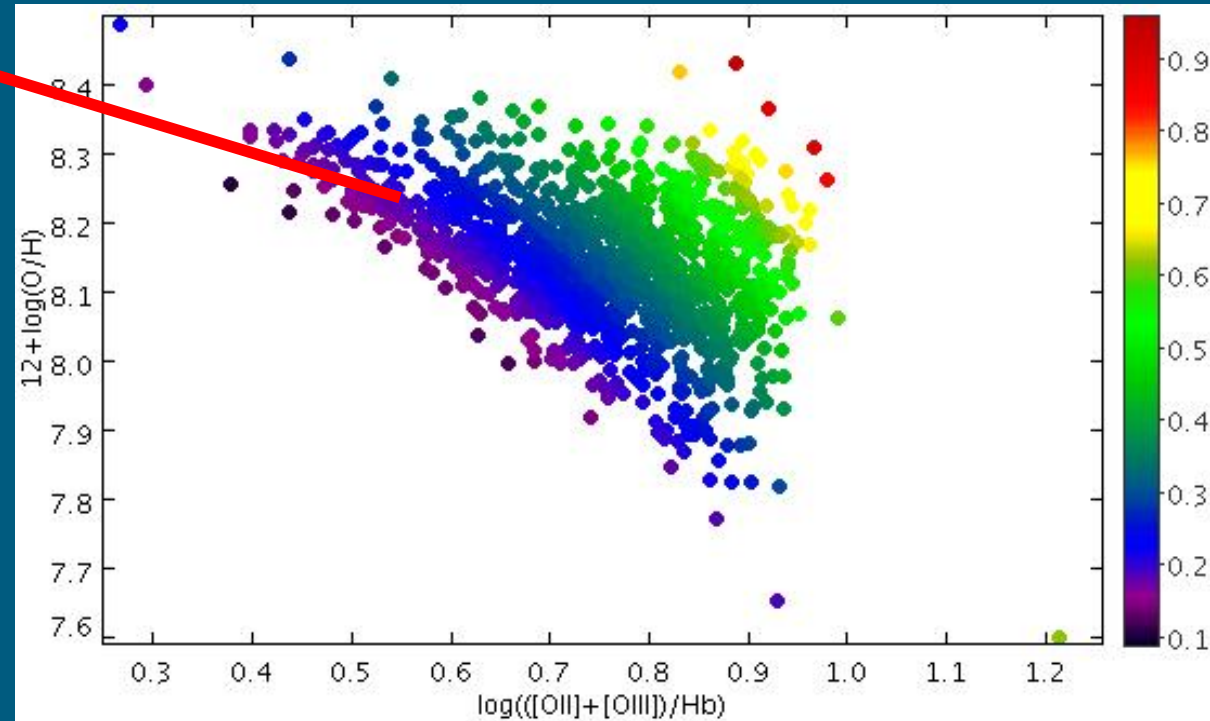
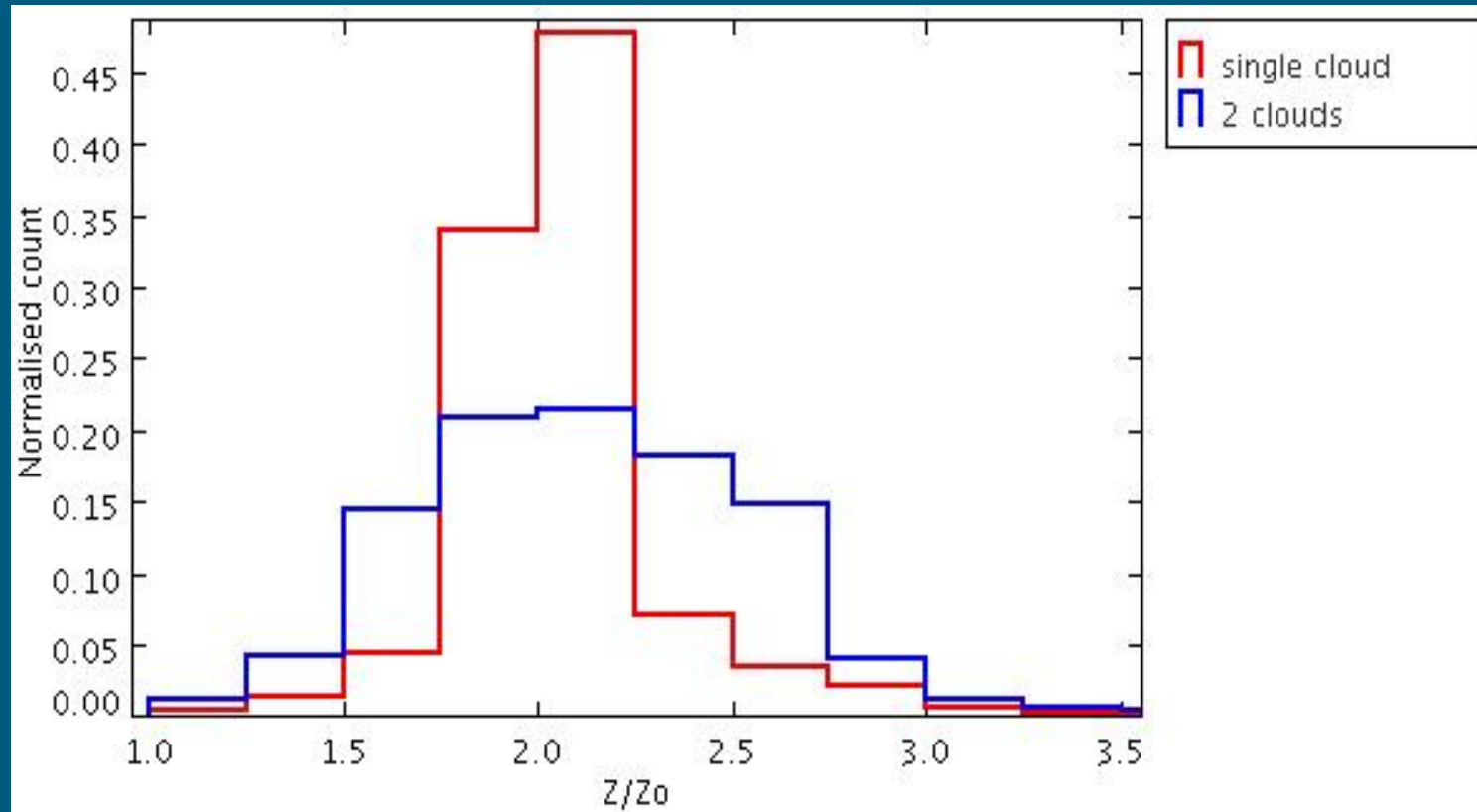


FIG. 12.—Family of $O/H = f(R_{23}, P)$ curves labeled by different values of the excitation parameter P , superimposed on the observational data. The high-metallicity H II regions with $0.0 < P < 0.3$ are shown by open squares, those with $0.3 < P < 0.6$ by plus signs, and those with $0.6 < P < 0.9$ by open circles. The low-metallicity H II regions with $0.5 < P < 0.7$ are shown by filled triangles, those with $0.7 < P < 0.9$ by crosses, and those with $0.9 < P < 1.0$ by filled circles.



The Oxygen abundances in gas are in the range $0.3-0.5 Z_{\square}$, assuming a maximum fraction of 40% of the total Oxygen in dust form (Silicate grains) the final Oxygen abundance range is $0.5-0.8 Z_{\square}$.

Seyfert 2 galaxies



Stellar population metallicities

Metallicity (and age) distribution of Seyferts, SF galaxies and NGs have been obtained using the results of STARLIGHT fit of the their continuum component.

Each component of the mixture of stellar populations (SPs) yielding the best fit of the observed continua is associated to a given age and metallicity.

Stellar population grid

The initial grid of stellar population is composed of the following combinations of age t and metallicity Z .

4 values of Z and 23 values of the age

	Age (yrs)	Z		Age (yrs)	Z		Age (yrs)	Z
1	$1.0 \cdot 10^6$	$4 \cdot 10^{-3}$	32	$4.0 \cdot 10^7$	$8 \cdot 10^{-3}$	63	$1.4 \cdot 10^9$	$2 \cdot 10^{-2}$
2	$3.2 \cdot 10^6$	$4 \cdot 10^{-3}$	33	$5.5 \cdot 10^7$	$8 \cdot 10^{-3}$	64	$2.5 \cdot 10^9$	$2 \cdot 10^{-2}$
3	$5.0 \cdot 10^6$	$4 \cdot 10^{-3}$	34	$1.0 \cdot 10^8$	$8 \cdot 10^{-3}$	65	$4.3 \cdot 10^9$	$2 \cdot 10^{-2}$
4	$6.6 \cdot 10^6$	$4 \cdot 10^{-3}$	35	$1.6 \cdot 10^8$	$8 \cdot 10^{-3}$	66	$6.3 \cdot 10^9$	$2 \cdot 10^{-2}$
5	$8.7 \cdot 10^6$	$4 \cdot 10^{-3}$	36	$2.9 \cdot 10^8$	$8 \cdot 10^{-3}$	67	$7.5 \cdot 10^9$	$2 \cdot 10^{-2}$
6	$1.0 \cdot 10^7$	$4 \cdot 10^{-3}$	37	$5.2 \cdot 10^8$	$8 \cdot 10^{-3}$	68	$1.0 \cdot 10^{10}$	$2 \cdot 10^{-2}$
7	$1.5 \cdot 10^7$	$4 \cdot 10^{-3}$	38	$9.0 \cdot 10^8$	$8 \cdot 10^{-3}$	69	$1.3 \cdot 10^{10}$	$2 \cdot 10^{-2}$
8	$2.5 \cdot 10^7$	$4 \cdot 10^{-3}$	39	$1.3 \cdot 10^9$	$8 \cdot 10^{-3}$	70	$1.0 \cdot 10^6$	$5 \cdot 10^{-2}$
9	$4.0 \cdot 10^7$	$4 \cdot 10^{-3}$	40	$1.4 \cdot 10^9$	$8 \cdot 10^{-3}$	71	$3.2 \cdot 10^6$	$5 \cdot 10^{-2}$
10	$5.5 \cdot 10^7$	$4 \cdot 10^{-3}$	41	$2.5 \cdot 10^9$	$8 \cdot 10^{-3}$	72	$5.0 \cdot 10^6$	$5 \cdot 10^{-2}$
11	$1.1 \cdot 10^8$	$4 \cdot 10^{-3}$	42	$4.3 \cdot 10^9$	$8 \cdot 10^{-3}$	73	$6.6 \cdot 10^6$	$5 \cdot 10^{-2}$
12	$1.6 \cdot 10^8$	$4 \cdot 10^{-3}$	43	$6.3 \cdot 10^9$	$8 \cdot 10^{-3}$	74	$8.7 \cdot 10^6$	$5 \cdot 10^{-2}$
13	$2.9 \cdot 10^8$	$4 \cdot 10^{-3}$	44	$7.5 \cdot 10^9$	$8 \cdot 10^{-3}$	75	$1.0 \cdot 10^7$	$5 \cdot 10^{-2}$
14	$5.1 \cdot 10^8$	$4 \cdot 10^{-3}$	45	$1.0 \cdot 10^{10}$	$8 \cdot 10^{-3}$	76	$1.5 \cdot 10^7$	$5 \cdot 10^{-2}$
15	$9.0 \cdot 10^8$	$4 \cdot 10^{-3}$	46	$1.3 \cdot 10^{10}$	$8 \cdot 10^{-3}$	77	$2.5 \cdot 10^7$	$5 \cdot 10^{-2}$
16	$1.3 \cdot 10^9$	$4 \cdot 10^{-3}$	47	$1.0 \cdot 10^6$	$2 \cdot 10^{-2}$	78	$4.0 \cdot 10^7$	$5 \cdot 10^{-2}$
17	$1.4 \cdot 10^9$	$4 \cdot 10^{-3}$	48	$3.2 \cdot 10^6$	$2 \cdot 10^{-2}$	79	$5.5 \cdot 10^7$	$5 \cdot 10^{-2}$
18	$2.5 \cdot 10^9$	$4 \cdot 10^{-3}$	49	$5.0 \cdot 10^6$	$2 \cdot 10^{-2}$	80	$1.0 \cdot 10^7$	$5 \cdot 10^{-2}$
19	$4.3 \cdot 10^9$	$4 \cdot 10^{-3}$	50	$6.6 \cdot 10^6$	$2 \cdot 10^{-2}$	81	$1.6 \cdot 10^8$	$5 \cdot 10^{-2}$
20	$6.3 \cdot 10^9$	$4 \cdot 10^{-3}$	51	$8.7 \cdot 10^6$	$2 \cdot 10^{-2}$	82	$2.9 \cdot 10^8$	$5 \cdot 10^{-2}$
21	$7.5 \cdot 10^9$	$4 \cdot 10^{-3}$	52	$1.0 \cdot 10^7$	$2 \cdot 10^{-2}$	83	$5.1 \cdot 10^8$	$5 \cdot 10^{-2}$
22	$1.0 \cdot 10^{10}$	$4 \cdot 10^{-3}$	53	$1.5 \cdot 10^7$	$2 \cdot 10^{-2}$	84	$9.0 \cdot 10^8$	$5 \cdot 10^{-2}$
23	$1.3 \cdot 10^{10}$	$4 \cdot 10^{-3}$	54	$2.5 \cdot 10^7$	$2 \cdot 10^{-2}$	85	$1.3 \cdot 10^9$	$5 \cdot 10^{-2}$
24	$1.0 \cdot 10^6$	$8 \cdot 10^{-3}$	55	$4.0 \cdot 10^7$	$2 \cdot 10^{-2}$	86	$1.4 \cdot 10^9$	$5 \cdot 10^{-2}$
25	$3.2 \cdot 10^6$	$8 \cdot 10^{-3}$	56	$5.5 \cdot 10^7$	$2 \cdot 10^{-2}$	87	$2.5 \cdot 10^9$	$5 \cdot 10^{-2}$
26	$5.0 \cdot 10^6$	$8 \cdot 10^{-3}$	57	$1.0 \cdot 10^8$	$2 \cdot 10^{-2}$	88	$4.3 \cdot 10^9$	$5 \cdot 10^{-2}$
27	$6.6 \cdot 10^6$	$8 \cdot 10^{-3}$	58	$1.6 \cdot 10^8$	$2 \cdot 10^{-2}$	89	$6.3 \cdot 10^9$	$5 \cdot 10^{-2}$
28	$8.7 \cdot 10^6$	$8 \cdot 10^{-3}$	59	$2.9 \cdot 10^8$	$2 \cdot 10^{-2}$	90	$7.5 \cdot 10^9$	$5 \cdot 10^{-2}$
29	$1.0 \cdot 10^7$	$8 \cdot 10^{-3}$	60	$5.1 \cdot 10^8$	$2 \cdot 10^{-2}$	91	$1.0 \cdot 10^{10}$	$5 \cdot 10^{-2}$
30	$1.5 \cdot 10^7$	$8 \cdot 10^{-3}$	61	$9.0 \cdot 10^8$	$2 \cdot 10^{-2}$	92	$1.3 \cdot 10^{10}$	$5 \cdot 10^{-2}$
31	$2.5 \cdot 10^7$	$8 \cdot 10^{-3}$	62	$1.3 \cdot 10^9$	$2 \cdot 10^{-2}$			

Table 1: List of stellar populations used for the evaluation of template spectra with age and metallicity Z .

Blending of the Stellar Populations (SP)

The global age t_g and metallicity Z_g of each galaxy has been estimated as the weighted average of ages and metallicity of the SPs according the percentage of light contributed to the spectrum:

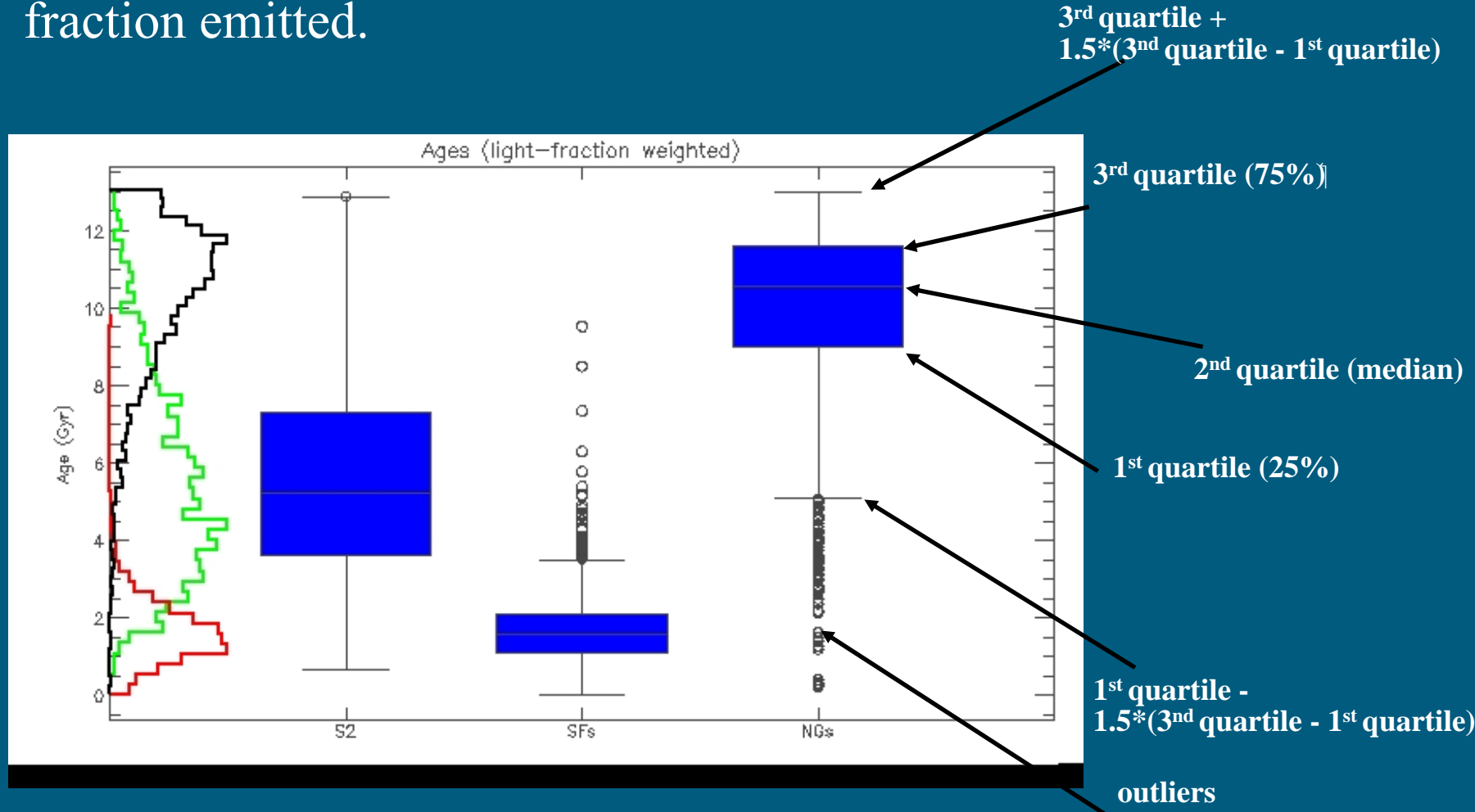
$$w_i = 1/f_i$$

where f_i is the fraction of light emitted by the i^{th} stellar population.

$$t_g = \frac{\sum_{i=0}^N w_i t_i}{\sum_{i=0}^N w_i} \quad Z_g = \frac{\sum_{i=0}^N w_i Z_i}{\sum_{i=0}^N w_i}$$

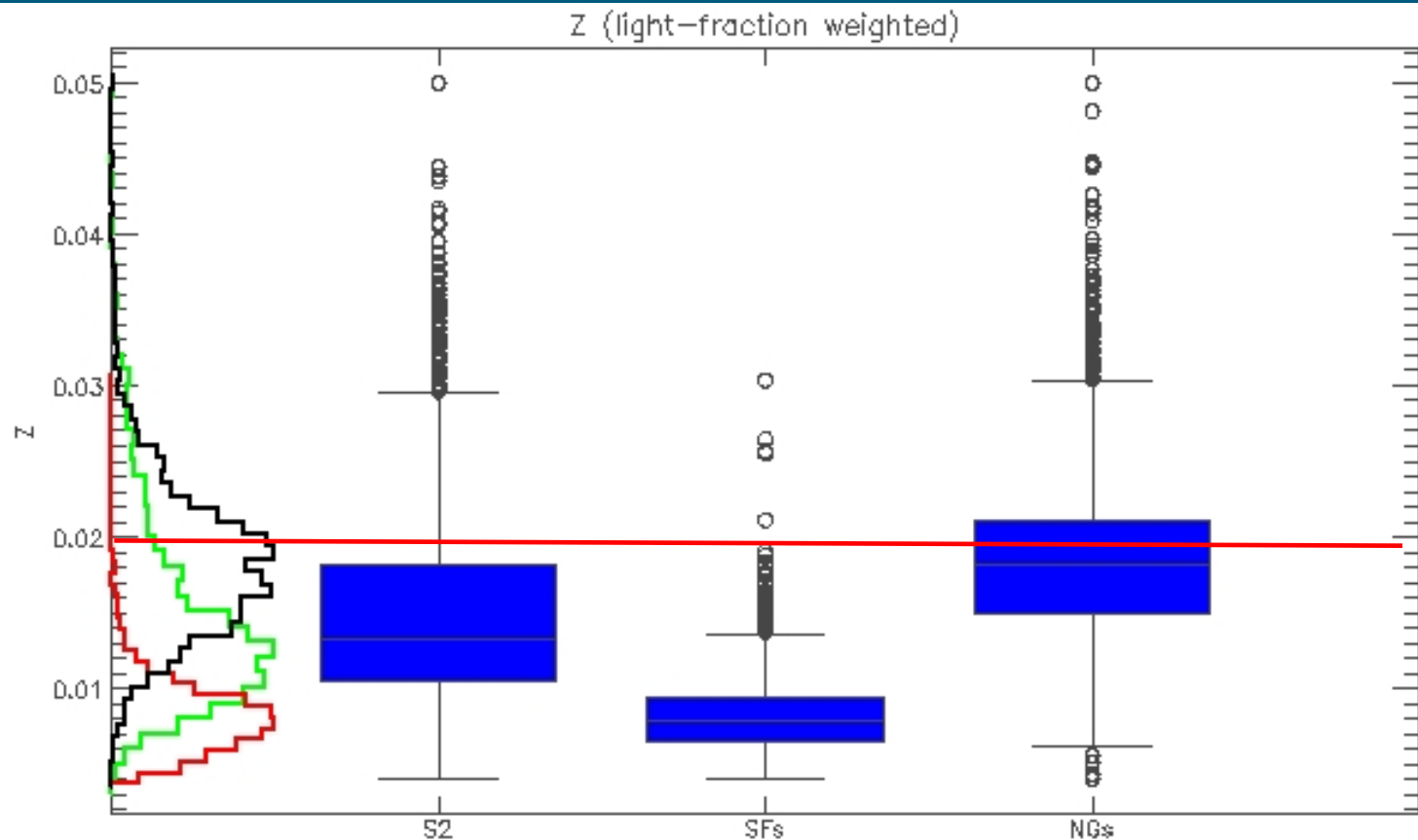
Age distribution

“Box and whisker” plots of the age distribution of S2, SFs and NGs obtained by weighing the single contributions by light fraction emitted.



Z distribution

“Box and whisker” plots of the Z distribution of S2, SFs and NGs obtained by weighing the single contributions by light fraction emitted.



Age and metallicity estimates from Mg₂

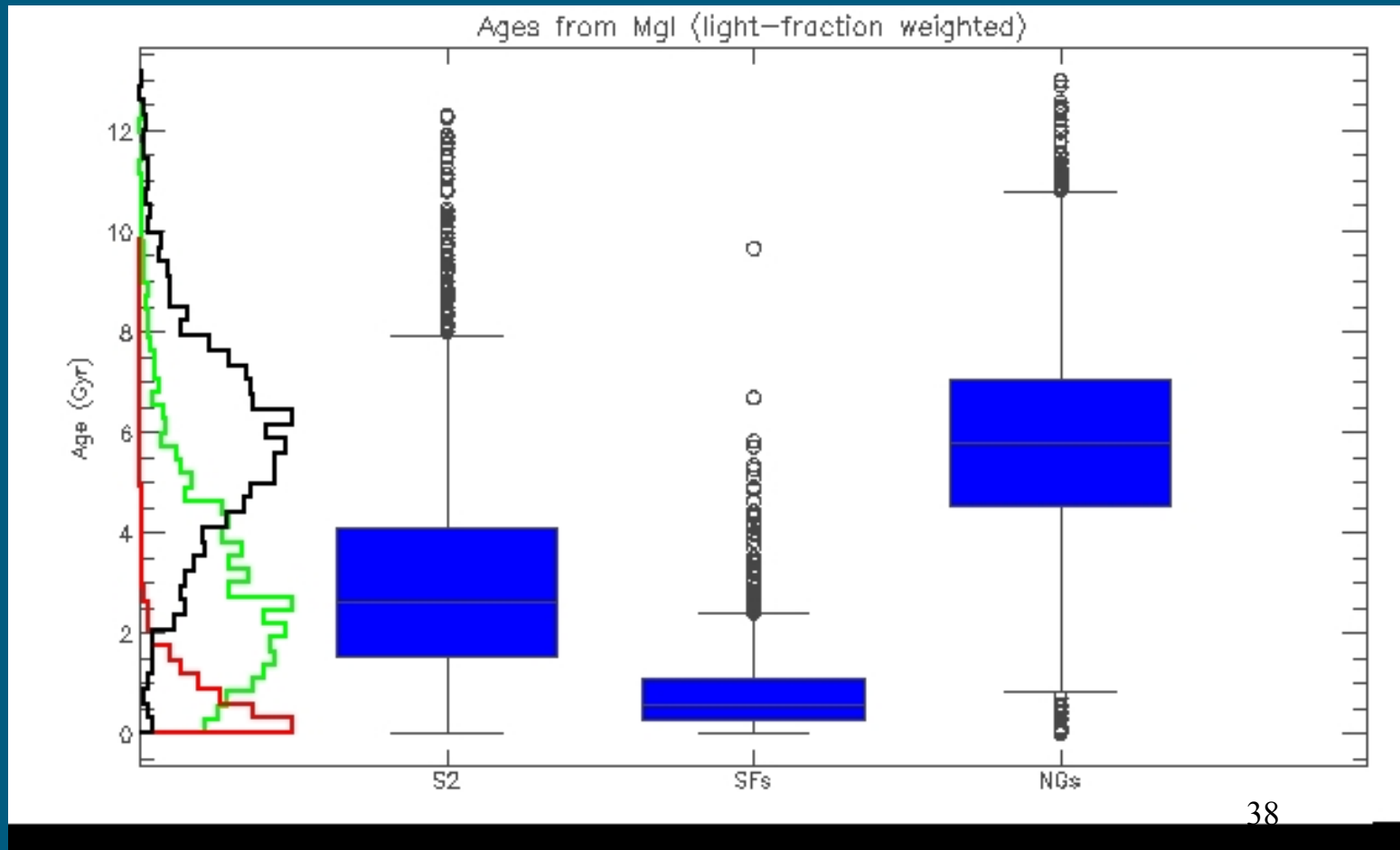
Faber et al. (1992) found a relation among the Mg₂ index and the age t and metallicity Z of a galaxy:

$$Mg_2 \sim 0.1 \left(\left(\frac{Z}{Z_{Sun}} \right) t [Gyr] \right)^{0.41}$$

Mg₂ index can be approximated by the e.w. of the Mg I absorption lines, measured and observed for all our spectra. So we can have estimates of Z and t using, in turn, only one of the parameters provided by STARLIGHT and letting the other free.

Age distribution from Mg₂

The three populations of galaxies appear to be, in general, younger than what we found using STARLIGHT parameters, even if the overall trend of the distribution is still present.



Z distribution from Mg₂

All the three samples show a smaller metallicity than before evaluated, even if the relative position of the peak of the distributions are the same.

